International Journal of Heat and Fluid Flow 30 (2009) 669–678

Contents lists available at ScienceDirect

International Journal of Heat and Fluid Flow

journal homepage: www.elsevier.com/locate/ijhff

Effects of inclination angle on natural convection in enclosures filled with Cu–water nanofluid

Eiyad Abu-Nada [a,*], Hakan F. Oztop [b]

[a] Department of Mechanical Engineering, Hashemite University, Zarqa 13115, Jordan
[b] Department of Mechanical Engineering, Firat University, Elazig TR-23119, Turkey

ARTICLE INFO

Article history:
Received 26 July 2008
Received in revised form 20 December 2008
Accepted 2 February 2009
Available online 18 March 2009

Keywords:
Nanofluids
Enclosure
Natural convection
Inclination angle

ABSTRACT

Effects of inclination angle on natural convection heat transfer and fluid flow in a two-dimensional enclosure filled with Cu-nanofluid has been analyzed numerically. The performance of nanofluids is tested inside an enclosure by taking into account the solid particle dispersion. The angle of inclination is used as a control parameter for flow and heat transfer. It was varied from = 0° to = 120°. The governing equations are solved with finite-volume technique for the range of Rayleigh numbers as $10^3 \leqslant Ra \leqslant 10^5$. It is found that the effect of nanoparticles concentration on Nusselt number is more pronounced at low volume fraction than at high volume fraction. Inclination angle can be a control parameter for nanofluid filled enclosure. Percentage of heat transfer enhancement using nanoparticles decreases for higher Rayleigh numbers.

1. Introduction

Analysis of natural convection heat transfer and fluid flow in enclosures has been extensively made using numerical techniques experiments because of its wide applications and interest in engineering such as nuclear energy, double pane windows, heating and cooling of buildings, solar collectors, electronic cooling, micro-electromechanical systems (MEMS). Further applications are listed by Ostrach (1988), Catton (1978), Bejan (1995), Khalifa Bdul-Jabbar (2001) and De Vahl Davis et al. (1983).

Elsherbiny (1996) made an experimental study to investigate the natural convection heat transfer in inclined rectangular enclosures. They indicated that the lowest heat transfer is formed for $\varphi = 180°$ (the cavity is heated from above). Bairi et al. (2007) performed a study on natural convection for high Rayleigh numbers using numerical and experimental techniques in rectangular inclined enclosures. They obtained a correlation between Nusselt and Rayleigh numbers and a minimal value for Nusselt numbers at $\varphi = 270^o$. Varol et al. (2008) investigated the effects of inclination angle on natural convection in an enclosure with corner heater. Lo et al. (2007) used a novel numerical solution algorithm based on a differential quadrature (DQ) method to simulate natural convection in an inclined cubic cavity using velocity–vorticity form of the Navier–Stokes equations. Aounallah et al. (2007) made a study on turbulent natural convection of air flow in a confined cavity with two differentially heated side walls is investigated numerically up to Rayleigh number of 1012. They analyzed the effect of the inclination angle and the amplitude of the undulation on turbulent heat transfer. Cianfrini et al. (2005) performed a study on natural convection in air filled, inclined enclosures with two adjacent walls heated and two opposite walls cooled. As indicated above that many researchers focused on effects of inclination angle on natural convection due to complexity of the flow. Aydin et al. (1999), Soong et al. (1996) and Lee and Lin (1995) made different applications for fluid filled inclined enclosures and found that inclination angle can be use a control parameter for heat and fluid flow.

An innovative technique to enhance heat transfer is by using nano-scale particles in the base fluid. Nanotechnology has been widely used in industry since materials with sizes of nanometers possess unique physical and chemical properties. Nano-scale particle added fluids are called as nanofluid which is firstly utilized by Choi (1995). Some numerical and experimental studies on nanofluids include thermal conductivity (Kang et al. (2006), convective heat transfer (Maiga et al., (2005), Abu-Nada, (2008) and Oztop and Abu-Nada (2008) boiling heat transfer and natural convection Xuan and Li (2000)) Polidori et al. (2007), Duangthongsuk and Wongwises (2008) and Jang and Choi (2004). Detailed review studies are published by Putra et al. (2003), Wang and Mujumdar (2006, 2007), and Trisaksri and Wongwises (2007). Recently, Daungthongsuk and Wongwises (2007) studied the influence of thermophysical properties of nanofluids on the convective heat transfer and summarized various models used in literature for predicting the thermophysical properties of nanofluids. They studied convective heat transfer coefficient in double-tube counter flow heat exchanger in the presence of TiO_2–water nanofluid.

* Corresponding author. Tel.: +962 390 3333; fax: +962 382 6613.
E-mail addresses: eiyad@hu.edu.jo, eiyad_abunada@yahoo.com (E. Abu-Nada).

0142-727X/$ - see front matter © 2009 Elsevier Inc. All rights reserved.
doi:10.1016/j.ijheatfluidflow.2009.02.001

Nomenclature

C_p	specific heat at constant pressure (kJ kg^{-1} K^{-1})
g	gravitational acceleration (m s^{-2})
H	height of the enclosure (m)
h	local heat transfer coefficient (W m^{-2} K^{-1})
h	dimensionless length of partial heater, $h\prime/H$
$h\prime$	length of heater (m)
Gr	Grash of number
k	thermal conductivity (W m^{-1} K^{-1})
Nu	Nusselt number, $Nu = hH/k$
Nu_{avg}	average Nusselt number
Pr	Prandtl number
qw	heat flux (W m^{-2})
Ra	Rayleigh number
T	dimensional temperature (K)
u, v	dimensional x and v components of velocity (m s^{-1})
U, V	dimensionless x and v components of velocity
W	length of the enclosure (m)
x, y	dimensionless coordinates
y_p	dimensionless center of heater
y'_p	center of location of heater (m)

Greek symbols

α	fluid thermal diffusivity (m^2 s^{-1})
β	thermal expansion coefficient (K^{-1})
ε	numerical tolerance
φ	nanoparticle volume fraction
ϕ	transport quantity
ν	kinematic viscosity (m^2 s^{-1})
θ	dimensionless temperature
Ψ	dimensionless stream function
ψ	dimensional stream function (m^2 s^{-1})
Ω	dimensionless vorticity
ω	dimensional vorticity (s^{-1})
ρ	density (kg m^{-3})
μ	dynamic viscosity(N s m^{-2})

Subscripts

avg	average
nf	nanofluid
f	fluid
H	hot
L	cold
s	Solid
w	wall
p	particle

Studies on natural convection using nanofluids are very limited and they are related with differentially heated enclosures. Hwang et al. (2007) investigated the buoyancy-driven heat transfer of water-based Al_2O_3 nanofluids in a rectangular cavity. They showed that the ratio of heat transfer coefficient of nanofluids to that of base fluid is decreased as the size of nanoparticles increases, or the average temperature of nanofluids is decreased. Khanafer et al. (2003) investigated the heat transfer enhancement in a two-dimensional enclosure utilizing nanofluids for various pertinent parameters. They tested different models for nanofluid density, viscosity, and thermal expansion coefficients. It was found that the suspended nanoparticles substantially increase the heat transfer rate any given Grashof number. Jou and Tzeng (2006) used nanofluids to enhance natural convection heat transfer in a rectangular enclosure. They conducted a numerical study using Khanafer's model. They indicated that volume fraction of nanofluids cause an increase in the average heat transfer coefficient.

The main aim of this work is to present the effects of inclination angle on flow field and temperature distribution in differentially heated and nanofluid filled enclosures. Based on above literature survey and to the author's knowledge, no previous study on effects of inclination angle on natural convection in nanofluid filled enclosure has not been studied yet.

2. Definition of model

Plotting of considered model is shown in Fig. 1 with coordinates. It is a two-dimensional square enclosure with an inclination angle. Its vertical wall has different isothermal temperature when inclination angle is zero. Remaining walls are adiabatic. The enclosure is filled with nanofluid which is Newtonian, incompressible and laminar.

3. Formulation

Fig. 1 shows a schematic diagram of the partially heated enclosure. The fluid in the enclosure is a water-based nanofluid containing copper nano particles. It is assumed that the base fluid (i.e. water) and the nanoparticles are in thermal equilibrium and no slip occurs between them. The thermo-physical properties of the nanofluid are given in Table 1. The left wall is maintained at a constant temperature (TH) higher than the right wall (TL). The thermo-physical properties of the nanofluid are assumed to be constant except for the density variation, which is approximated by the Boussinesq model.

The governing equations for the laminar and steady state natural convection in terms of the stream function-vorticity formulation are:

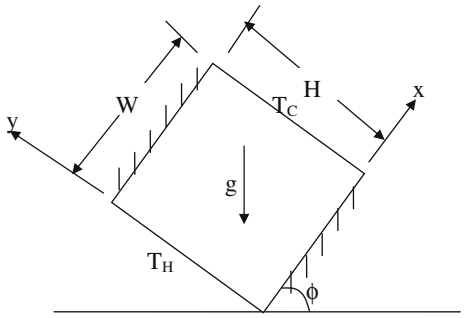

Fig. 1. Schematic of inclined enclosure.

Table 1
Thermophysical properties of pure fluid and nanoparticles.

Physical properties	Fluid phase (Water)	Cu
C_p (J/kg K)	4179	385
ρ (kg/m^3)	997.1	8933
K (W/mK)	0.613	400
$\alpha \times 10^7$ (m^2/s)	1.47	1163.1
$\beta \times 10^{-5}$ (1/K)	21	1.67

Vorticity

$$\frac{\partial}{\partial x'}\left(\omega\frac{\partial \Psi}{\partial y'}\right)-\frac{\partial}{\partial y'}\left(\omega\frac{\partial \Psi}{\partial x'}\right)=\frac{\mu_{nf}}{\rho_{nf}}\left(\frac{\partial \omega}{\partial x'^2}+\frac{\partial \omega}{\partial y'^2}\right)+\frac{(\varphi\rho_s\beta_s+(1-\varphi)\rho_f\beta_f)}{\rho_{nf}}g\left(\frac{\partial T}{\partial x'}\cos\phi-\frac{\partial T}{\partial y'}\sin\phi\right) \quad (1)$$

Energy

$$\frac{\partial}{\partial x'}\left(T\frac{\partial \Psi}{\partial y'}\right)-\frac{\partial}{\partial y'}\left(T\frac{\partial \Psi}{\partial x'}\right)=\frac{\partial}{\partial x'}\left[\alpha_{nf}\frac{\partial T}{\partial x'}\right]+\frac{\partial}{\partial y'}\left[\alpha_{nf}\frac{\partial T}{\partial y'}\right] \quad (2)$$

Kinematics

$$\frac{\partial^2 \Psi}{\partial x'^2}+\frac{\partial^2 \Psi}{\partial y'^2}=-\omega \quad (3)$$

$$\alpha_{nf}=\frac{k_{eff}}{(\rho c_p)_{nf}} \quad (4)$$

The effective density of the nanofluid is given as

$$\rho_{nf}=(1-\varphi)\rho_f+\varphi\rho_s \quad (5)$$

The heat capacitance of the nanofluid is expressed as Abu-Nada (2008) and Khanafer et al. (2003):

$$(\rho c_p)_{nf}=(1-\varphi)(\rho c_p)_f+\varphi(\rho c_p)_s \quad (6)$$

The effective thermal conductivity of the nanofluid is approximated by the Maxwell–Garnetts model:

$$\frac{k_{nf}}{k_f}=\frac{k_s+2k_f-2\varphi(k_f-k_s)}{k_s+2k_f+\varphi(k_f-k_s)} \quad (7)$$

The use of this equation is restricted to spherical nanoparticles where it does not account for other shapes of nanoparticles. This model is found to be appropriate for studying heat transfer enhancement using nanofluids (Akbarinia and Behzadmehr, 2007; Abu-Nada, 2008; Maiga et al., 2005). The viscosity of the nanofluid can be approximated as viscosity of a base fluid μ_f containing dilute suspension of fine spherical particles and is given by Brinkman (1952):

$$\mu_{nf}=\frac{\mu_f}{(1-\varphi)^{2.5}} \quad (8)$$

The radial and tangential velocities are given by the following relations, respectively:

$$u=\frac{\partial \Psi}{\partial y'} \quad (9)$$

$$v=-\frac{\partial \Psi}{\partial x'} \quad (10)$$

The following dimensionless groups are introduced:

$$x=\frac{x'}{H};\quad y=\frac{y'}{H};\quad \Omega=\frac{\omega H^2}{\alpha_f};\quad \Psi=\frac{\Psi}{\alpha_f};\quad V=\frac{vH}{\alpha_f};\quad U=\frac{uH}{\alpha_f},\quad \theta=\frac{T-T_L}{T_H-T_L} \quad (11)$$

By using the dimensionless parameters the equations are written as

$$\frac{\partial}{\partial x}\left(\Omega\frac{\partial \Psi}{\partial y}\right)-\frac{\partial}{\partial y}\left(\Omega\frac{\partial \Psi}{\partial x}\right)=\left[\frac{Pr}{(1-\varphi)^{0.25}\left((1-\varphi)+\varphi\frac{\rho_s}{\rho_f}\right)}\right]\left(\frac{\partial^2 \Omega}{\partial x^2}+\frac{\partial^2 \Omega}{\partial y^2}\right)+GrPr^2\left[\frac{1}{\frac{(1-\varphi)}{\varphi}\frac{\rho_f}{\rho_s}+1}\frac{\beta_s}{\beta_f}+\frac{1}{\frac{\varphi}{(1-\varphi)}\frac{\rho_f}{\rho_s}+1}\right]\left(\frac{\partial T}{\partial x}\cos\phi-\frac{\partial T}{\partial y}\sin\phi\right) \quad (12)$$

$$\frac{\partial}{\partial x}\left(\theta\frac{\partial \Psi}{\partial y}\right)-\frac{\partial}{\partial y}\left(\theta\frac{\partial \Psi}{\partial x}\right)=\frac{\partial}{\partial x}\left(\lambda\frac{\partial \theta}{\partial x}\right)+\frac{\partial}{\partial y}\left(\lambda\frac{\partial \theta}{\partial y}\right) \quad (13)$$

$$\frac{\partial^2 \Psi}{\partial x^2}+\frac{\partial^2 \Psi}{\partial y^2}=-\Omega \quad (14)$$

$$\lambda=\frac{\frac{k_{nf}}{k_f}}{(1-\varphi)+\varphi\frac{(\rho c_p)_s}{(\rho c_p)_f}} \quad (15)$$

Grashof and Prandtl numbers are given in Eq. 16, respectively.

$$Gr=\frac{g\beta H^3(T_H-T_L)}{v^2},\quad Pr=\frac{v}{\alpha} \quad (16)$$

Rayleigh number is

$$Ra=\frac{g\beta H^3(T_H-T_L)}{v\alpha} \quad (17)$$

The dimensionless radial and tangential velocities are given as, respectively:

$$U=\frac{\partial \Psi}{\partial y} \quad (18)$$

$$V=-\frac{\partial \Psi}{\partial x} \quad (19)$$

The dimensionless boundary conditions are written as

$$\left.\begin{array}{l}\text{1-On the left wall i.e., } x=0,\ \Psi=0,\ \Omega=-\frac{\partial^2 \Psi}{\partial x^2},\ \theta=1\\ \text{2-On the right wall i.e., } x=1,\ \Psi=0,\ \Omega=-\frac{\partial^2 \Psi}{\partial x^2},\ \theta=0\\ \text{3-On the top and bottom walls}: \Psi=0,\ \Omega=-\frac{\partial^2 \Psi}{\partial y^2},\ \frac{\partial \theta}{\partial y}=0\end{array}\right\} \quad (20)$$

4. Numerical analysis

Equations (12)–(14) with corresponding boundary conditions given in Eq. 20, are solved using the finite-volume approach (Patankar, 1980; Versteeg and Malalasekera, 1995). The diffusion term in the vorticity and energy equations is approximated by a second-order central difference scheme which gives a stable solution. Furthermore, a second-order upwind differencing scheme is adopted for the convective terms. The algebraic finite-volume equations for the vorticity and energy equations are written into the following form:

$$a_P\phi_P=a_E\phi_E+a_W\phi_W+a_N\phi_N+a_S\phi_S+b \quad (21)$$

where P, W, E, N, S denote cell location, west face of the control volume, east face of the control volume, north face of the control volume and south face of the control volume respectively. Similar expression is also used for the kinematics equation where only central difference is used for the discritization at the cell P of the control volume. The resulted algebraic equations are solved using successive over/under relaxation method. Successive under relaxation was used due to the non-linear nature of the governing equations especially for the vorticity equation at high Rayleigh numbers. The convergence criterion is defined by the following expression:

$$\varepsilon=\frac{\sum_{j=1}^{j=M}\sum_{i=1}^{i=N}|\phi^{n+1}-\phi^n|}{\sum_{j=1}^{j=M}\sum_{i=1}^{i=N}|\phi^{n+1}|}<10^{-6} \quad (22)$$

where ε is the tolerance; M and N are the number of grid points in the x and y directions, respectively.

An accurate representation of vorticity at the surface is the most critical step in the stream function-vorticity formulation. A second-

order accurate formula is used for the vorticity boundary condition. For example, the vorticity at the bottom wall is expressed as

$$\Omega = -\frac{(8\Psi_{1,j} - \Psi_{2,j})}{2(\Delta y)^2} \tag{23}$$

Algebraic equations are solved using successive under/over relaxation method. After solving Ψ, Ω, and T, further useful quantities are obtained. For example, the Nusselt number can be expressed as

$$Nu = \frac{hH}{k_f} \tag{24}$$

The heat transfer coefficient is expressed as

$$h = \frac{q_w}{T_H - T_L} \tag{25}$$

The thermal conductivity is expressed as

$$k_{nf} = -\frac{q_w}{\partial T/\partial x} \tag{26}$$

By substituting Eqs. (25) and (26) and Eq. (7) into Eq. (24), and using the dimensionless quantities, the Nusselt number on the left wall is written as

$$Nu = -\left(\frac{k_{nf}}{k_f}\right)\frac{\partial T}{\partial x} \tag{27}$$

The average Nusselt number is defined as

$$Nu_{avg} = \int_0^1 Nu(y)dy \tag{28}$$

A 1/3rd Simpson's rule of integration is used to evaluate Eq. (28).

5. Grid testing and code validation

An extensive mesh testing procedure was conducted to guarantee a grid independent solution. Seven different mesh combinations were used for the case of $Ra = 10^5$, $Pr = 0.7$, and zero inclination angle. The present code was tested for grid independence by calculating the average Nusselt number on the left wall. It is found that a grid size of 51×51 ensures a grid independent solution. The converged value ($Nu = 4.644$) was compared to other known values reported by other researchers as shown in Fig. 2a. Therefore, the converged value compares very well with other values obtained in literature.

The present numerical solution is further validated by comparing the present code results for $Ra = 10^5$ and $Pr = 0.70$ and zero inclination angle against the experiment of Krane and Jessee (1983) and numerical simulation of Khanafer et al. (2003). It is clear that the present code is in good agreement with other work reported in literature as shown in Fig. 2b.

6. Results and discussion

A numerical analysis has been conducted to investigate the effects of inclination angle on a Cu–water nanofluid filling a two-dimensional inclined square enclosure. The enclosure is differentially heated and the other two opposite walls are adiabatic. Calculations were made for various values of volume fraction of nanoparticle ($0 \leqslant \varphi \leqslant 0.1$), inclination angles ($0^\circ \leqslant \leqslant 120^\circ$) and Rayleigh numbers ($10^3 \leqslant Ra \leqslant 10^5$). The thermophysical properties of pure fluid and copper nanoparticles are listed in Table 1.

Fig. 3a–c shows the effects of Rayleigh number on streamlines (on the left) and isotherms (on the right) for $\phi = 0.1$. The figure presents a comparison for flow field and temperature distribution of

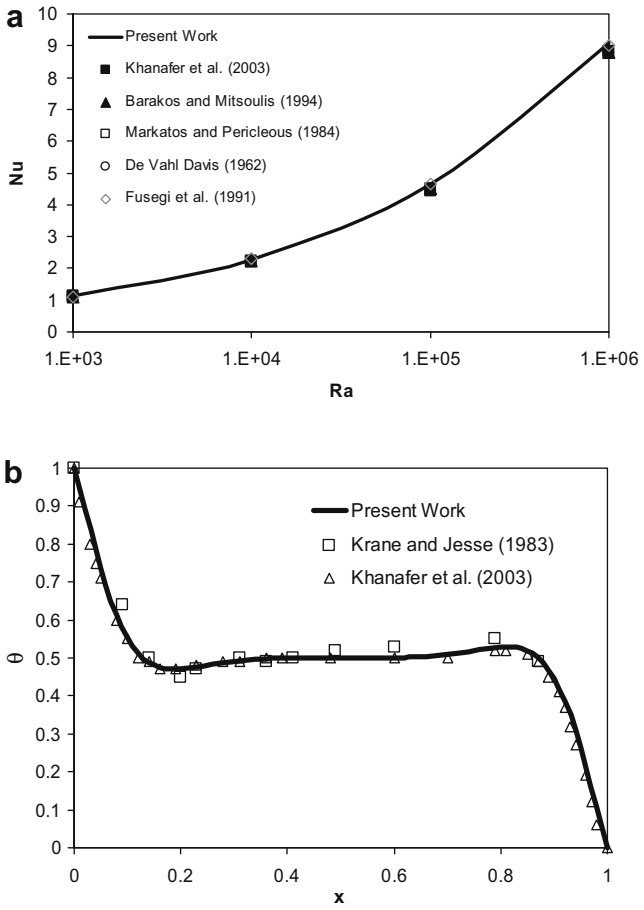

Fig. 2. (a) Nusselt number versus *Ra* number and comparison with other published works, and (b) comparison between present work and other published data for the temperature distribution on the left wall ($Ra = 105$, $Pr = 0.7$, $\varphi = 0^\circ$).

nanofluid (smooth lines) and pure fluid (dashed lines). Also, this figure is presented to compare the obtained result with literature (Khanafer et al., 2003). A singular cell is formed at low Rayleigh number and the shape of the main cell is circular. As shown in the figure, the shape of the cell becomes ellipsoidal with the increasing of Rayleigh number. The addition of nanoparticle affects the diameter of the cell. In all cases, the flow rotates in clockwise direction. Moreover, Fig. 3 illustrates how the thickness of thermal boundary layer next to the heated wall is influenced by the addition of nanoparticles. This sensitivity of thermal boundary layer thickness to volume fraction of nanoparticles is related to the increased thermal conductivity of the nanofluid. In fact, higher values of thermal conductivity are accompanied by higher values of thermal diffusivity. The high value of thermal diffusivity cause a drop in the temperature gradients and accordingly increases the boundary thickness as demonstrated in Fig. 3b. This increase in thermal boundary layer thickness reduces the Nusselt number, however, according to Eq. (27), the Nusselt number is a multiplication of temperature gradient and the thermal conductivity ratio (conductivity of the of the nanofluid to the conductivity of the base fluid). Since the reduction in temperature gradient due to the presence of nanoparticles is much smaller than thermal conductivity ratio therefore an enhancement in Nusselt is taking taken place by increasing the volume fraction of nanoparticles. The enhancement in Nusselt number will be addressed later in detail in this discussion section.

Fig. 4a–d illustrates the streamlines and isotherms at different inclination angles for $Ra = 10^5$ and $\phi = 0.1$. Again, this figure makes

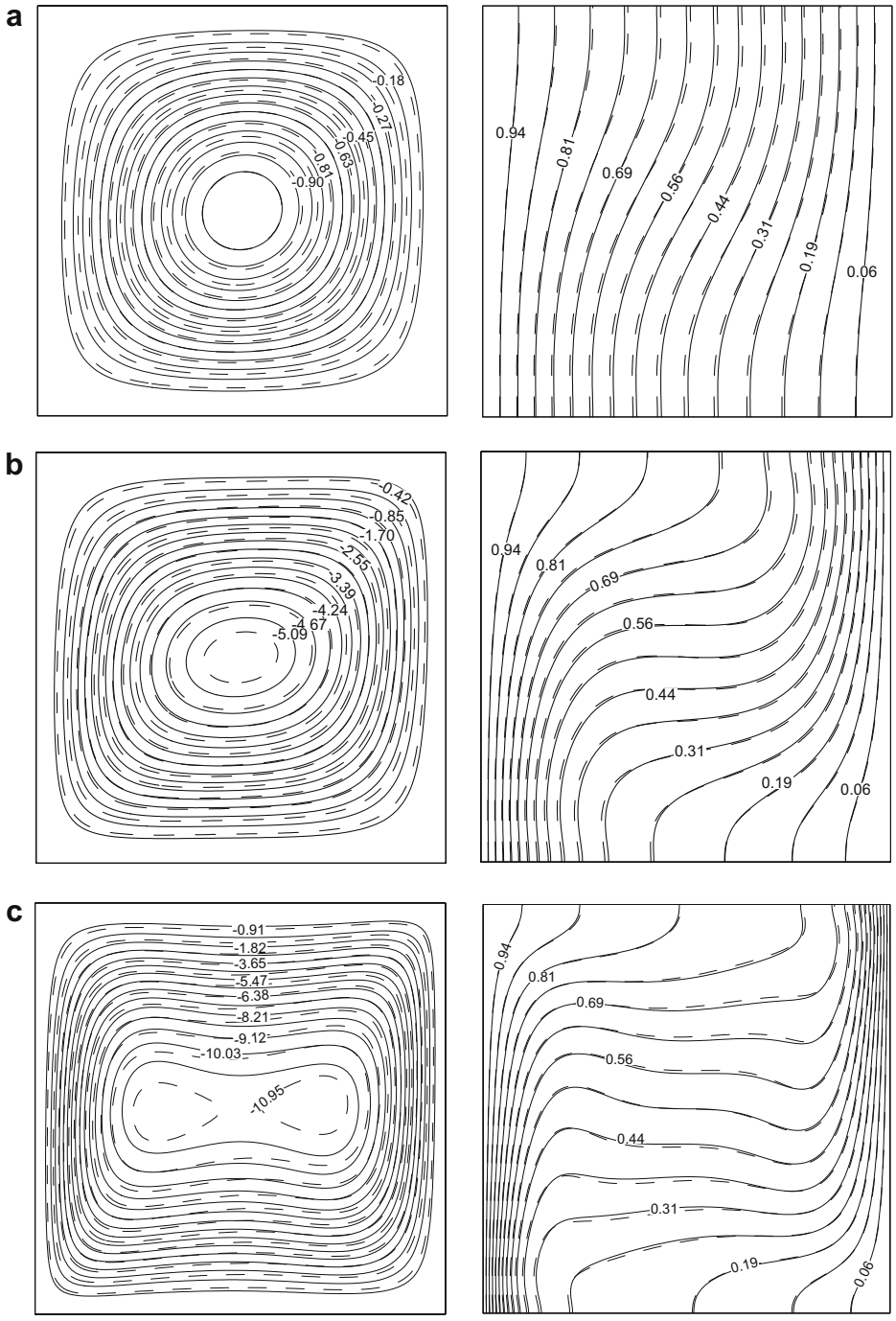

Fig. 3. Streamlines (left) and isotherms (right) for $\varphi = 0°$ and $\phi = 0.1$, (a) $Ra = 10^3$ ($\psi_{min} = -1.156$), (b) $Ra = 10^4$ ($\psi_{min} = -5.228$), and (c) $Ra = 10^5$ ($\psi_{min} = -11.22$), (pure fluid (dashed lines —), lines (nanofluids)).

a comparison between Cu–water nanofluid and pure fluid. It is observed that the shape of the main cell is sensitive to the inclination angle and addition of nanoparticles. Also, isotherms indicate the addition of nanoparticle becomes more effective for = 90°. In this case, Rayleigh–Bénard type flow is formed inside the enclosure because of the existence of a vertical thermal gradient in the cavity. The appearance of the plume is believed to be the reason for the more enhancement in heat transfer for = 90°. More discussion on this behavior will be addressed later when studying Fig. 8. Rotation direction of flow completely changes for = 120° from clockwise to counterclockwise.

Effects of volume fraction on flow fields and temperature distribution are displayed in Fig. 5a and b for $Ra = 10^5$ and $\varphi = 30°$. As indicated in the literature (Khanafer et al., 2003), the velocity components of nanofluid increase as a result of an increase in the energy transport in the fluid with the increasing of volume fraction. Thus, the dimension of main cell becomes smaller with increasing of volume fraction of nanofluid. The absolute values of streamfunctions indicate that the strength of flow increases with increasing of volume fraction of nanofluid.

Fig. 6a–e presents the variation of Nusselt number against Rayleigh number for different inclination angles. Three different particle concentrations are used as $\varphi = 0$, 0.05, and 0.1. The figure shows that the effect of nanoparticles concentration on Nusselt number is more pronounced at low Rayleigh number than at high Rayleigh number. This is related to the conduction dominated mechanism

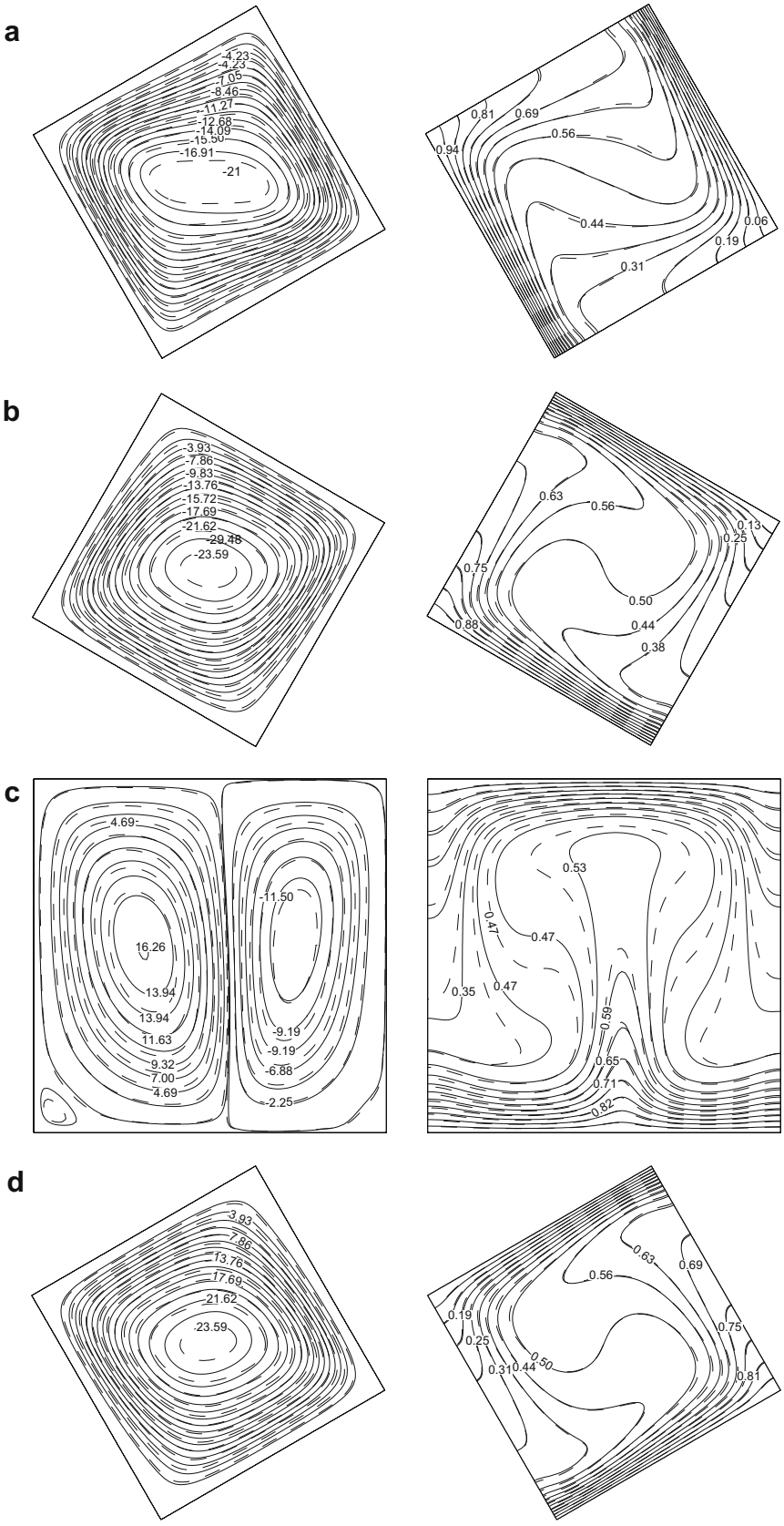

Fig. 4. Streamlines (on the left) and isotherms (on the right) for $Ra = 10^5$ and $\phi = 0.1$, (a) $\varphi = 30°$, ($\psi_{min} = -17.42$ (pure fluid)), $\psi_{min} = -22.55$ (nanofluid)), (b) $\varphi = 60°$, ($\psi_{min} = -24.08$ (pure fluid), $\psi_{min} = -31.44$ (nanofluid)), (c) $\varphi = 90°$, ($\psi_{min} = -16.13$ (nanofluid)), ($\psi_{max} = 20.88$ (nanofluid)), (d) $\varphi = 120°$, ($\psi_{max} = 26$ (purefluid), $\psi_{max} = 31.44$ (nanofluid)), (pure fluid (dashed lines —), lines (nanofluids)).

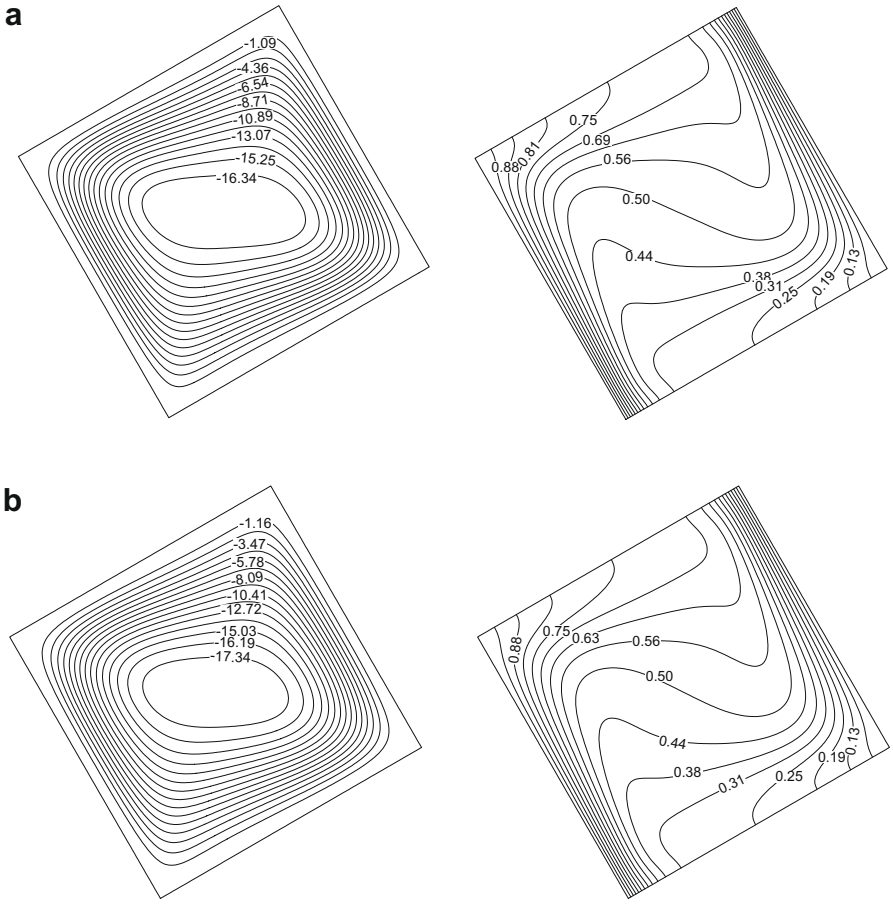

Fig. 5. Streamlines (on the left) and isotherms (on the right) for $Ra = 10^5$ and $\varphi = 30°$, (a) $= 0$, ($\psi_{min} = -17.42$), b) $= 0.05$, ($\psi_{min} = -18.49$).

for heat transfer at low Rayleigh number compared to convection mechanism at higher Rayleigh number. Therefore, the effect of high conductive nanoparticles on heat transfer becomes more significant at low Rayleigh number. However, the buoyancy forces increase and they overcome the viscous forces and the heat transfer is dominated by convection at high Rayleigh number. Also, it is interesting to note that at high nanoparticles concentration the Brinkman model of viscosity makes the fluid more viscous which explains the relatively smaller difference between the Nusselt number for the cases of $Ra = 1 \times 10^4$ and $Ra = 1 \times 10^5$ compared to the difference between $Ra = 1 \times 10^4$ and $Ra = 1 \times 10^3$.

The inclination angle affects the heat transfer. Globally, heat transfer decreases with inclination angle and the lowest heat transfer is formed for $= 90°$. Fig. 7 shows the variation of mean Nusselt number with Rayleigh number for different inclination angles. Heat transfer is increased with increasing of Rayleigh number monotonically. It is demonstrated that the case of inclination angle of 90° has the lowest Nusselt number due to the low velocity encountered at this angle; see Fig. 8, where the vertical velocity is plotted at the middle of the heated wall ($y = 0.5$) for $= 0.1$ and $Ra = 10^5$. Also, Fig. 7 shows the maximum Nusselt number occurs for the case of inclination angle of 30° due to the increase of flow velocity at this angle as shown in Fig. 8. Also, Fig. 7 shows that conduction regime prevailed for $Ra = 1000$ and then the mean Nusselt number started to deviate from the value of $Nu \cong 1$.

Fig. 9 is presented to show the variation of the local Nusselt number along the heated wall for the case of inclination angle of 90°. Fig. 9 shows that the minimum value of Nusselt number is located around the centerline of the plume. The temperature gradient at the heated wall is a minimum in the plume region which leads to minimum value of Nusselt number in the plume region. The temperature gradient is a minimum in the plume region because the thermal boundary layer thickness in the plume region becomes very large. This is accompanied by a reduction in temperature gradients. Also, Fig. 9 shows that the addition of nanoparticles causes the Nusselt number to increase.

Fig. 10 illustrates the variation of local Nusselt number along the heated wall at different inclination angle for $= 0.1$. As seen from the figure, local Nusselt number decreases along the lower half of the hot wall for the values of inclination angle from $= 0°$ to $= 60°$. However, the Nusselt number enhances on the top portion of the wall. A wavy trend is observed for $= 90°$ due to formation of Rayleigh–Bénard type flow inside the enclosure. Thus, two maximum points were formed at this angle but their values are lower than that of other values of inclination angles due to the reduced value of velocity as shown in Fig. 8.

The previous discussions indicate that generally heat transfer enhances with addition of nanoparticle. To estimate the enhancement of heat transfer between the case of $\varphi = 0.1$ and the pure fluid (base fluid) case, the enhancement is defined as

$$E = \frac{Nu(\varphi = 0.1) - Nu(basefluid)}{Nu(basefluid)} \times 100\% \tag{29}$$

Enhancement of heat transfer ($\varphi = 0.1$) is plotted versus inclination angle at different Rayleigh numbers in Fig. 11. For the whole range of Rayleigh numbers, the figure illustrates that enhancement of heat transfer is almost constant up to $= 60°$. Also, the percentage of heat transfer enhancement decreases with increasing of Rayleigh number for all inclination angles. It is an interesting observation that

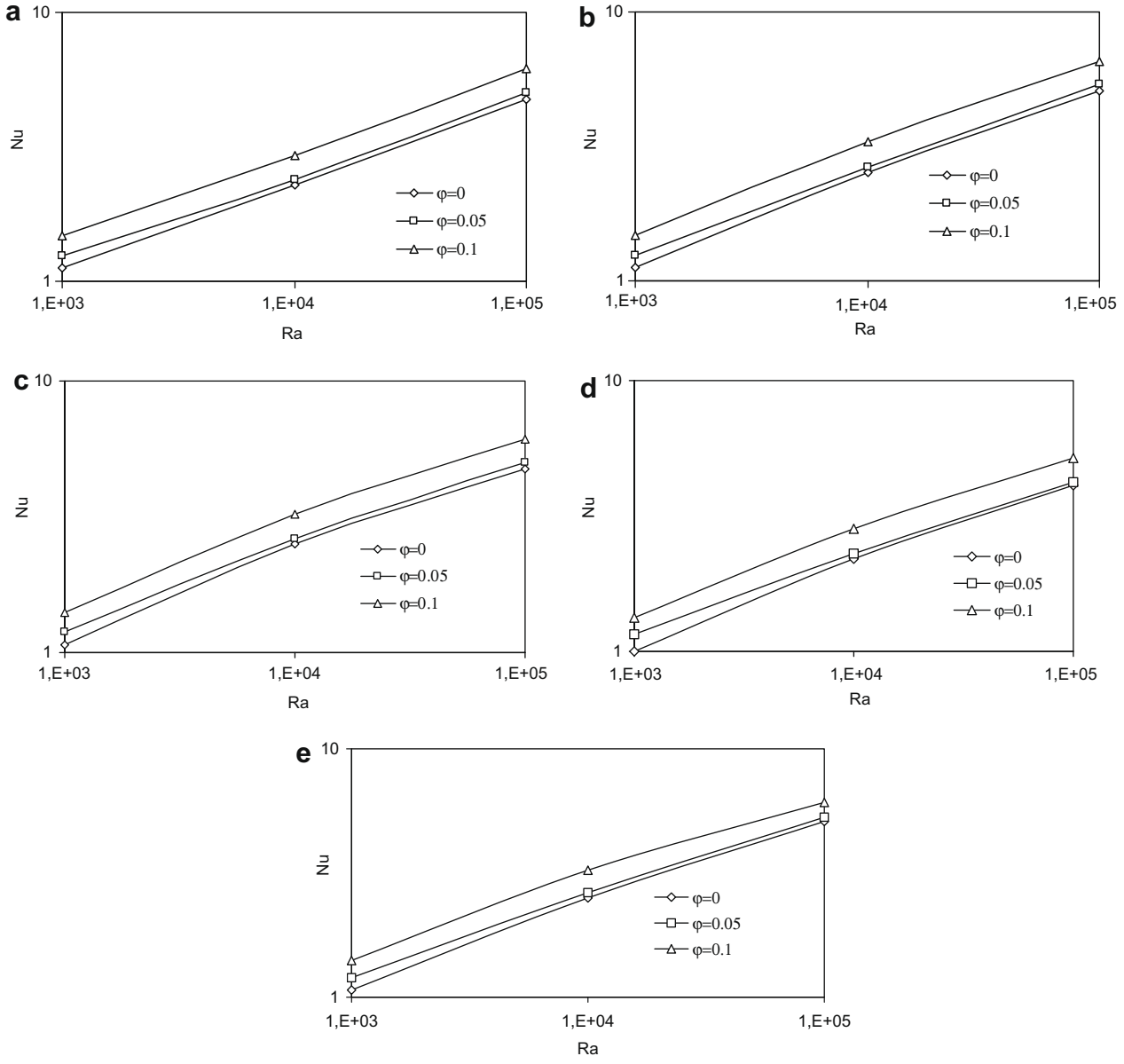

Fig. 6. Variation of mean Nusselt numbers with Rayleigh numbers at different values of volume fraction for different inclination angles (a) = 0°, (b) = 30°, (c) = 60°, (d) = 90°, (e) = 120°.

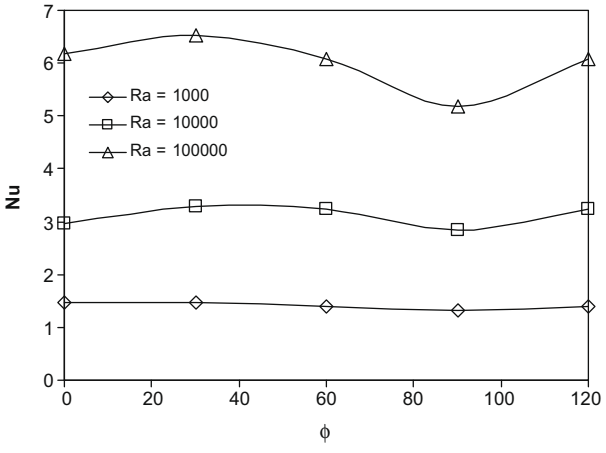

Fig. 7. Variation of mean Nusselt numbers with inclination angles for $\varphi = 0.1$.

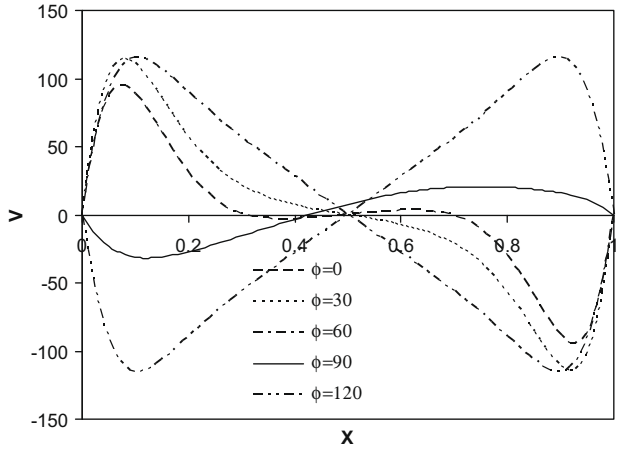

Fig. 8. Velocity profiles along the middle of hot wall for different inclination angle for $\varphi = 0.1$ and $Ra = 10^5$.

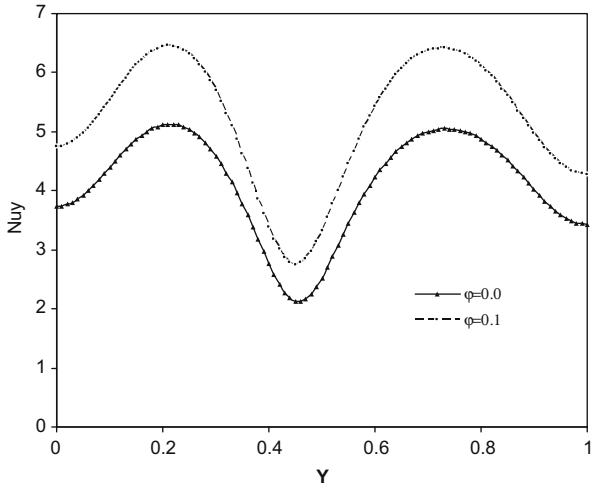

Fig. 9. Variation of Nusselt number along the heated wall for $\phi = 90^{\circ}$.

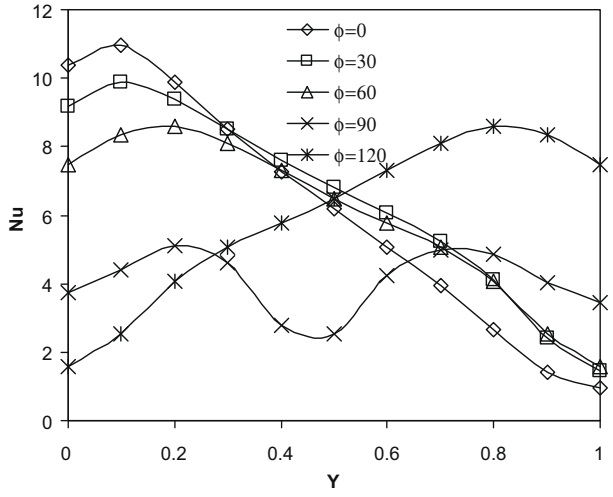

Fig. 10. Variation of local Nusselt number along the heated wall for = 0.1 at different inclination angles.

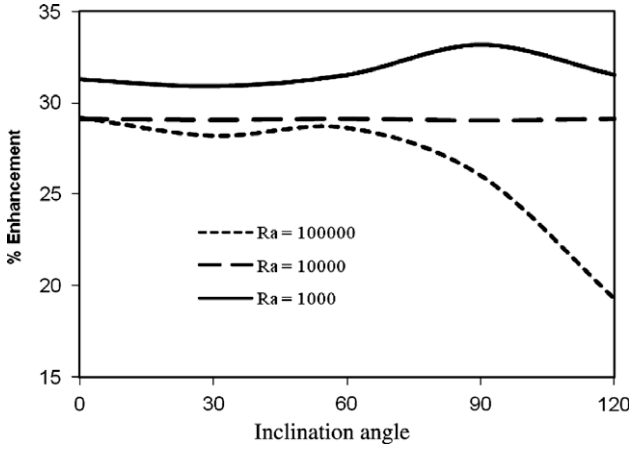

Fig. 11. Ratio of enhancement of heat transfer due to addition of nanoparticles.

the enhancement in heat transfer for $Ra = 1 \times 10^4$ is the same for all inclination angles. Also, for $Ra = 10^5$, the enhancement in heat transfer is reduced by increasing the inclination angle.

7. Conclusions

In this paper the influence of inclination angle and volume fraction of nanoparticle have been studied for a square enclosure. Copper–water was used as nanofluid. Results have clearly indicated that the addition of copper nanoparticles has produced a remarkable enhancement on heat transfer with respect to that of the pure fluid. Heat transfer enhances with increasing of Rayleigh number almost linearly but the effect of nanoparticles concentration on Nusselt number is more pronounced at low Rayleigh number than at high Rayleigh number. Inclination angle of the enclosure is proposed a control parameter for fluid flow and heat transfer. It was found that lower heat transfer is formed for = 90°. But higher values of volume fraction become insignificant from the fluid flow point of view at this inclination angle. Effects of inclination angle on percentage of heat transfer enhancement become insignificant at low Rayleigh number but it decreases the enhancement of heat transfer with nanofluid. Finally, the inclination angle is a good control parameter for both pure and nanofluid filled enclosures.

References

Abu-Nada, E., 2008. Application of nanofluids for heat transfer enhancement of separated flows encountered in a backward facing step. Int. J. Heat Fluid Flow 29, 242–249.

Akbarinia, A., Behzadmehr, A., 2007. Numerical study of laminar mixed convection of a nanofluid in horizontal curved tubes. Appl. Therm. Eng. 27, 1327–1337.

Aounallah, M., Addad, Y., Benhamadouche, S., Imine, O., Adjlout, L., Laurence, D., 2007. Numerical investigation of turbulent natural convection in an inclined square cavity with a hot wavy wall. Int. J. Heat Mass Transfer 50, 1683–1693.

Aydin, O., Unal, A., Ayhan, T., 1999. A numerical study on buoyancy-driven flow in an inclined square enclosure heated and cooled on adjacent walls. Numer. Heat Transfer Part A 36, 585–589.

Bairi, A., Laraqi, N., Garcia de Maria, J.M., 2007. Numerical and experimental study of natural convection in tilted parellelepipedic cavities for large Rayleigh numbers. Exp. Therm. Fluid Sci. 31, 309–324.

Bejan, A., 1995. Convective Heat Transfer, second ed. Wiley, New York.

Brinkman, H.C., 1952. The viscosity of concentrated suspensions and solutions. J. Chem. Phys. 20, 571–581.

Catton, I., 1978. Natural convection in enclosures. In: Proceedings of the Sixth International Heat Transfer Conference, 6.

Choi, U.S., 1995. Enhancing thermal conductivity of fluids with nanoparticles. In: Siginer, D.A., Wang, H.P. (Eds.), Developments and Applications of Non-Newtonian Flows, FED, vol. 231, 66, pp. 99–105.

Cianfrini, C., Corcione, M., Dell'Omo, P.P., 2005. Natural convection in tilted square cavities with differentially heated opposed walls. Int. J. Therm. Sci. 44, 441–451.

Daungthongsuk, W., Wongwises, S., 2007. A critical review of convective heat transfer nanofluids. Renew. Sust. Eng. Rev. 11, 797–817.

De Vahl Davis, G., Jones, I.P., 1983. Natural convection in a square cavity: a bench mark numerical solution. Int. J. Numer. Meth. Fluid 3, 227–248.

Duangthongsuk, W., Wongwises, S., 2008. Effect of thermophysical properties models on the predicting of the convective heat transfer coefficient for low concentration nanofluid. Int. Commun. Heat Mass Transfer 35, 1320–1326.

Elsherbiny, S.M., 1996. Free convection in inclined air layers heated from above. Int. J. Heat Mass Transfer 39, 3925–3930.

Hwang, K.S., Ji-Hwan, L., Jang, S.P., 2007. Buoyancy-driven heat transfer of water-based Al_2O_3 nanofluids in a rectangular cavity. Int. J. Heat Mass Transfer 50, 4003–4010.

Jang, S.P., Choi, S.U.S., 2004. Free convection in a rectangular cavity (Benard convection) with nanofluids. In: Proceedings of the IMECE, Anaheim, California, USA.

Jou, R.Y., Tzeng, S.C., 2006. Numerical research of nature convective heat transfer enhancement filled with nanofluids in rectangular enclosures. Int. Commun. Heat Mass Transfer 33, 727–736.

Kang, H.U., Kim, S.H., Oh, J.M., 2006. Estimation of thermal conductivity of nanofluid using experimental effective particle volume. Exp. Heat Transfer 19, 181–191.

Khalifa Bdul-Jabbar, N., 2001. Natural convective heat transfer coefficient – a review, II. Isolated vertical and horizontal surfaces. Energy Convers. Manage. 42, 505–517.

Khanafer, K., Vafai, K., Lightstone, M., 2003. Buoyancy-driven heat transfer enhancement in a two-dimensional enclosure utilizing nanofluids. Int. J. Heat Mass Transfer 46, 3639–3653.

Krane, R., Jessee, J., 1983. Some detailed field measurements for a natural convection flow in a vertical square enclosure. In: Proceedings of the First ASME–JSME Thermal Engineering Joint Conference, 1, pp. 323–329.

Lee, T., Lin, T.F., 1995. Three dimensional natural convection of air in an inclined cubic cavity. Numer. Heat Transfer Part A 27, 681–703.

Lo, D.C., Young, D.L., Murugesan, K., Tsai, C.C., Gou, M.H., 2007. Velocity–vorticity formulation for 3D natural convection in an inclined cavity by DQ method. Int. J. Heat Mass Transfer 50, 479–491.

Maiga, S.E.B., Palm, S.J., Nguyen, C.T., Roy, G., Galanis, N., 2005. Heat transfer enhancement by using nanofluids in forced convection flows. Int. J. Heat Fluid Flow 26, 530–546.

Ostrach, S., 1988. Natural convection in enclosures. J. Heat Transfer 110, 1175–1190.

Oztop, H.F., Abu-Nada, E., 2008. Numerical study of natural convection in partially heated rectangular enclosure filled with nanofluids. Int. J. Heat Fluid Flow 29 (5), 1326–1336.

Patankar, S.V., 1980. Numerical Heat Transfer and Fluid Flow. Hemisphere Publishing Corporation, Taylor and Francis Group, New York.

Polidori, G., Fohanno, S., Nguyen, C.T., 2007. A note on heat transfer modeling of Newtonian nanofluids in laminar free convection. Int. J. Therm. Sci. 46, 739–744.

Putra, N., Roetzel, W., Das, S.K., 2003. Natural convection of nano-fluids. Heat Mass Transfer 39, 775–784.

Soong, C.Y., Tzeng, P.Y., Chiang, D.C., Sheu, T.S., 1996. Numerical study on mode transition of natural convection in differentially heated inclined enclosures. Int. J. Heat Mass Transfer 39, 2869–2882.

Trisaksri, V., Wongwises, S., 2007. Critical review of heat transfer characteristics of nanofluids. Renew. Sust. Energy Rev. 11, 512–523.

Varol, Y., Oztop, H.F., Koca, A., Ozgen, F., 2008. Natural convection and fluid flow in inclined enclosure with a corner heater. Appl. Therm. Eng. doi:10.1016/j.applthermaleng.2008.02.033.

Versteeg, H.K., Malalasekera, W., 1995. An Introduction to Computational Fluid Dynamic: The Finite Volume Method. John Wiley & Sons Inc, New York.

Wang, X.-Q., Mujumdar, A.S., 2007. Heat transfer characteristics of nanofluids: a review. Int. J. Therm. Sci. 46, 1–19.

Wang, X.-Q., Mujumdar, A.S., Yap, C., 2006. Free convection heat transfer in horizontal and vertical rectangular cavities filled with nanofluids. In: International Heat Transfer Conference IHTC-13, Sydney, Australia.

Xuan, Y., Li, Q., 2000. Heat transfer enhancement of nanofluids. Int. J. Heat Fluid Flow 21, 58–64.